Inorganic Chemistry

Article

pubs.acs.org/IC

Molybdenum 17- and 18-Electron Bis- and Tris(Butadiene) Complexes: Electronic Structures, Spectroscopic Properties, and Oxidative Ligand Substitution Reactions

Gerald C. Stephan, Christian Näther, Gerhard Peters, and Felix Tuczek*

Institut für Anorganische Chemie, Christian Albrechts Universität zu Kiel, Max-Eyth-Straße 2, D-24098 Kiel, Germany

Supporting Information

ABSTRACT: New results on the electronic structures, spectroscopic properties, and reactivities of the molybdenum tris(butadiene) and tris(2,3-dimethylbutadiene) complexes $[Mo(bd)_3]$ ($\mathbf{1}^{bd}$) and $[Mo(dmbd)_3]$ ($\mathbf{1}^{dmbd}$), respectively, are reported. Importantly, the metal ligand bonding interaction can be weakened by oxidizing the metal center with ferrocenium salts. The addition of the bidentate phosphine ligand 1,2-bis(diphenylphosphino)ethane then leads to a new type of stable 17-electron complex, $[Mo(dmbd)_2(dppe)](X)$ ($\mathbf{2}$; X = BF_4^-, PF_6^-, BPh_4^-), where one of the butadiene ligands is exchanged by a chelating phosphine. Reduction of the cationic complexes $\mathbf{2}$ generates the corresponding 18-electron complex $[Mo(dmbd)_2(dppe)]$ ($\mathbf{3}$), thus establishing a new strategy for ligand substitution reactions in $[Mo(bd)_3]$ complexes via one-electron oxidized intermediates. The new heteroleptic molybdenum complexes are characterized by X-ray structure analysis; vibrational, NMR, and EPR spectroscopy; and electrochemistry. DFT calculations are performed to explain the structural and specroscopic trends observed experimentally. For compound $\mathbf{1}^{bd}$, a normal coordinate analysis is presented, providing additional information on the bonding situation in this type of complex.

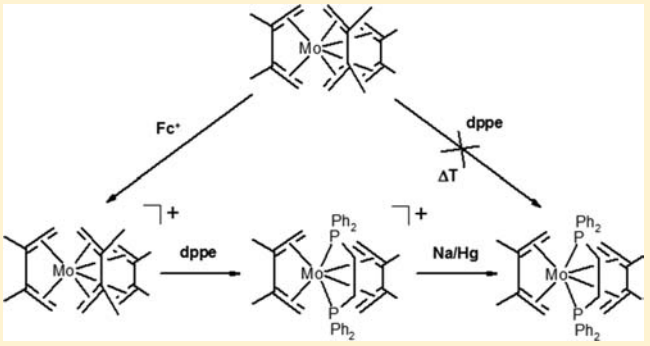

I. INTRODUCTION

Due to their unusual trigonal-prismatic structure, molybdenum complexes with a tris(1,3-butadiene) coordination are interesting compounds in the field of group 6 transition metal chemistry.[1,2] In comparison to other homoleptic molybdenum compounds like $[Mo(CO)_6]$, $[Mo(arene)_2]$, or $[Mo(PMe_3)_6]$, the reactivity of these systems is less explored. $[Mo(CO)_6]$, e.g., undergoes various substitution reactions with nitriles, phosphines, arenes, and vinylketones.[3−5] Depending on the reaction conditions, up to four CO ligands can be substituted. Similar reactivities can be observed for bis(arene) compounds leading to different types of half-sandwich complexes.[6] Besides ligand exchange reactions of $[Mo(CO)_6]$ or $[Mo(arene)_2]$ complexes under thermal or photochemical reaction conditions, also exchange reactions under oxidizing conditions are known.[7,8] For the highly reactive molybdenum complex $[Mo(PMe_3)]_6$, a wide range of exchange reactions especially with heterocycles has been described and analyzed in detail.[9−11]

The few reactions known for molybdenum and tungsten tris(1,3-butadiene) complexes have been described by Wilke et al. It was found that $[Mo(bd)_3]$ and $[W(bd)_3]$ undergo substitution reactions of the butadiene (bd) ligands against COT and CO accompanied by a trimerization of butadiene to cyclododecatriene.[12] Furthermore, the compounds were tested as catalysts for polymerization and metathesis reactions.[13] Nevertheless, none of the well-defined exchange reactions which are routinely used for other molybdenum complexes have been established for the butadiene compounds to date.

The reason for these findings is the special bonding situation in $[Mo(bd)_3]$: due to backbonding from the molybdenum center, an equalization of the C−C bond lengths occurs in the butadiene ligands. This delocalized bonding mode causes a high stability of the molybdenum butadiene complexes and renders these systems inert toward exchange reactions with electron-donating ligands like phosphines under thermal reaction conditions. Kaupp et al. have analyzed this bonding situation employing X-ray analysis and theoretical calculations,[2] providing theoretical evidence for a significant transfer of charge from the (formally zerovalent) molybdenum center to the (formally neutral) butadiene ligands. This way, resonance structures with a Mo(IV) center and two dinegative butadiene ligands were found to provide the best description of the actual charge distribution.

In this paper, we describe how vibrational spectroscopy can be used to obtain further insight into the electronic structure of this class of compounds. Furthermore, we present our first results on the reactivities of the homoleptic complexes tris(butadiene)molybdenum $[Mo(bd)_3]$ ($\mathbf{1}^{bd}$) and tris(2,3-dimethylbutadiene)molybdenum $[Mo(dmbd)_3]$ ($\mathbf{1}^{dmbd}$). Im-

Received: January 18, 2013
Published: April 29, 2013

 © 2013 American Chemical Society dx.doi.org/10.1021/ic400145f | Inorg. Chem. 2013, 52, 5931−5942

Table 1. Selected Crystallographic Data and Results of the Structure Refinement for $[Mo(dmbd)_2(dppe)](BPh_4)$ ($\mathbf{2}^{BPh4}$), $[Mo(dmbd)_2(dppe)]$ (**3**), and $[MoF_2(dppe)_2](BF_4)$ (**4**)

compound	$[Mo(dmbd)_2(dppe)]BPh_4$ ($\mathbf{2}^{BPh4}$)	$[Mo(dmbd)_2(dppe)]$ (**3**)	$[MoF_2(dppe)_2](BF_4)$ (**4**)
empirical formula	$C_{62}H_{64}BMoP_2$	$C_{38}H_{44}MoP_2$	$C_{52}H_{48}BF_6MoP_4$
fw g mol^{-1}	977.82	658.61	1017.53
temp/K	170(2)	170(2)	170(2)
cryst syst	triclinic	monoclinic	monoclinic
space group	$P\bar{1}$	$P2_1/n$	Cc
unit cell dimensions			
a/Å	11.856(1)	9.711(1)	9.867(1)
b/Å	13.758(1)	12.454(1)	22.528(2)
c/Å	16.281(2)	26.280(2)	21.175(2)
α/deg	89.96(1)		
β/deg	85.09(11)	91.70(1)	92.68(1)
γ/deg	71.29(1)		
vol/Å^3	2505.1(3)	3177.0(3)	4701.5(5)
Z	2	4	4
D_{calcd}/Mg/m^3	1.296	1.377	1.438
μ/mm^{-1}	0.366	0.539	0.475
θ range/deg	2.28−26.02	2.22−28.05	2.41−28.06
index ranges	$-14 \le h \le 14$	$-12 \le h \le 12$	$-12 \le h \le 13$
	$-16 \le k \le 16$	$-16 \le k \le 16$	$-29 \le k \le 29$
	$-20 \le l \le 20$	$-34 \le l \le 34$	$-27 \le l \le 27$
reflns collected	24750	39264	23978
independent reflns	9632	7658	11122
R_{int}	0.0557	0.0399	0.0370
reflns with $[I > 2\sigma(I)]$	7840	6640	10612
params	600	372	578
GoF on F^2	1.054	1.033	1.029
R1 $[I > 2\sigma(I)]$	0.0494	0.0268	0.0324
wR2 (all data)	0.1381	0.0704	0.0817
δF (e/Å^3)	2.126/−0.878	0.384/−0.559	0.457/−0.554

portantly, we find that the metal ligand bonding interaction can be weakened by oxidizing the metal center with a ferrocenium salt. The addition of the bidentate phosphine ligand 1,2-bis(diphenylphosphino)ethane then leads to the formation of a new type of stable cationic complex, $[Mo(dmbd)_2(dppe)](X)$ (**2**; X = BF_4^-, PF_6^-, BPh_4^-), where one of the butadiene ligands is exchanged by the chelating phosphine. In contrast to other mononuclear molybdenum 17-electron compounds which are very sensitive, the molybdenum complexes with butadiene−phosphine coordination exhibit a high stability and can be stored under air as a solid or in solution over months without any signs of decomposition. As a side product of the reaction, the butadiene-free molybdenum complex $[MoF_2(dppe)_2](BF_4)$ (**4**) was isolated. Reduction of the 17-electron complexes **2** leads to the corresponding neutral compound $[Mo(dmbd)_2(dppe)]$ (**3**), thus establishing a new strategy for ligand substitution reactions in $[Mo(bd)_3]$ complexes via one-electron oxidized intermediates. A comparable molybdenum complex, $[Mo(bd)_2(PMe_3)_2]$, has already be synthesized by Brookhart et al., employing an exchange reaction based on the highly reactive complex $[Mo(PMe_3)_6]$.[14] Moreover, two related monophosphine (PEt_3, PMe_2Ph) bis(1,3-butadiene) complexes have been synthesized by Galindo et al. starting from molybdenum(0) alkene or dinitrogen complexes.[15] An interesting aspect of the PEt_3 containing complex $[Mo(bd)_2(PEt_3)_2]$ was the fact that it could be synthesized based on a dimerization of ethylene.

The new complexes $[Mo(dmbd)_2(dppe)](X)$ (**2**; X = BF_4^-, PF_6^-, BPh_4^-) and $[Mo(dmbd)_2(dppe)]$ (**3**) described in this study are characterized by X-ray structure analysis, spectroscopy, and electrochemical methods. Furthermore, the electronic structure of complexes **2** and **3** is determined and compared to the electronic structure of $\mathbf{1}^{bd}$ analyzed before.[2]

II. EXPERIMENTAL SECTION

General Methods. All reactions were performed under an inert gas atmosphere using Schlenk techniques. The solvents were dried and freshly distilled under inert gas. All other reagents were used without further purification. $[Mo(bd)_3]$ ($\mathbf{1}^{bd}$) and $[Mo(dmbd)_3]$ ($\mathbf{1}^{dmbd}$) were prepared using literature procedures.[26] IR spectra were obtained from KBr pellets using a Bruker IFS v66/S FT-IR spectrometer. Raman spectra were obtained on a Bruker IFS 66/CS NIR FT-Raman spectrometer. The setup involves a 350 mW Nd:YAG laser with an excitation wavelength of 1064 nm. NMR spectra were recorded on a Bruker Avance 400 pulse Fourier transform spectrometer operating at a ^{1}H frequency of 400.13 MHz (^{31}P 161.98 MHz, ^{13}C 106.62) using a 5 mm inverse triple-resonance probe head. References as substitutive standards: H_3PO_4 85% pure, $\delta(^{31}P)$ 0 ppm. Elemental analyses were performed with a Euro Vector Euro EA 3000. The magnetic properties were determined with a Bruker B-SU 20 Faraday balance containing a Sartorius 4411 balance at 15 kGs.

The electrochemical measurements (cyclovoltammetry, difference-pulse voltammetry) were performed with an EG&G PAR Model 273 A potentiostat using a platinum-knob working electrode, a silver-rod counterelectrode, and a platinum rod auxiliary electrode. The setup was controlled by the EG&G PAR M270 software. For referencing, ferrocene was added as an internal standard.

X-Ray Structure Analysis. Intensity data were collected using a STOE imaging plate diffraction system (IPDS-1) with Mo Kα radiation (λ = 0.71073 Å). All structures were solved with direct methods using SHELXS-97, and refinement was performed against F^2

dx.doi.org/10.1021/ic400145f | Inorg. Chem. 2013, 52, 5931−5942

using SHELXL-97. All non-hydrogen atoms were refined anisotropically. The hydrogen atoms were positioned with idealized geometries (methyl H atoms allowed to rotate but not to tip) and were refined using a riding model. The absolute structure of compound **4** was determined and is in agreement with the selected setting (Flack x-parameter: −0.024(18)). The crystal of compound $\mathbf{2}^{\mathbf{BPh4}}$ was slightly nonmerohedrically twinned, but both individuals could not be separated successfully. Selected crystal data and results of the structure refinements are summarized in Table 1.

CCDC-934953 ($\mathbf{2}^{\mathbf{BPh4}}$), CCDC-934954 (**3**), and CCDC-934955 (**4**) contain the supplementary crystallographic data for this paper, which can be obtained free of charge from the Cambridge Crystallographic Data Center via www.ccdc.cam.uk/data_request.cif.

Density Functional Calculations. DFT calculations were performed for the complexes $[Mo(bd)_3]$ (**1**), $[Mo(dmbd)_2(dppe)]^+$ (**2**), and $[Mo(dmbd)_2(dppe)]$ (**3**) using Becke's three parameter hybrid functional with the correlation functional of Lee, Young, and Parr (B3LYP).[16] The LANL2DZ basis set was used for the calculations. It applies Dunning/Huzinaga full double-ζ basis functions on the first row and Los Alamos effective core potentials plus DZ functions on all other atoms.[17,18] All computational procedures were used as implemented in the Gaussian 03 package.[19] Wave functions were plotted with GaussView03.[20]

Normal Coordinate Analysis. Normal coordinate calculations were performed using the QCPE computer program by Peterson and McIntosh.[21] It involves solutions of the secular equation **GFL** = **ΛL** by the diagonalization procedure of Miyazawa. The calculations are based on a general valence force field, and the force constants are refined using the nonlinear optimization of the simplex algorithm according to Nelder and Mead.[22] The f-matrix that derives from the DFT calculation has its force constants in Cartesian coordinates. These Cartesian coordinates were transformed to internal coordinates using the program REDONG.[23]

Preparation of [Mo(dmbd)(dppe)](X) (X= PF_6^- ($\mathbf{2}^{\mathbf{PF6}}$), BF_4^- ($\mathbf{2}^{\mathbf{BF4}}$), and BPh_4^- ($\mathbf{2}^{\mathbf{BPh4}}$)). $\mathbf{2}^{\mathbf{PF6}}$: 10 mL of THF was added to a mixture of 185 mg (0.54 mmol) of $[Mo(dmbd)_3]$ ($\mathbf{1}^{\mathbf{dmbd}}$), 185 mg (0.56 mmol) of $FcPF_6$, and 216 mg (0.54 mmol) of dppe. The suspension turned green after a few minutes and was stirred for 1 h. The addition of 10 mL of *n*-hexane to the mixture causes a complete precipitation of the product. The green solid was filtered from the yellow-orange solution, washed with 2 × 5 mL *n*-hexane, and dried under vacuum conditions. Yield: 350 mg (0.44 mmol, 87%). Anal. Calcd for $C_{38}H_{44}P_3F_6Mo$: C, 56.81%; H, 5.48%. Found: C, 57.10%; H, 4.49%.

$\mathbf{2}^{\mathbf{BF4}}$: The compound has been prepared in analogy to compound $\mathbf{2}^{\mathbf{PF6}}$ (based on 0.5 mmol of $[Mo(dmbd)_3]$). Yield: 270 mg (0.36 mmol, 72%). Anal. Calcd for $C_{38}H_{44}P_2F_4BMo$: C, 61.23%; H, 5.90%. Found: C, 60.93%; H, 5.91%.

$\mathbf{2}^{\mathbf{BPh4}}$: The compound has been prepared in analogy to compound $\mathbf{2}^{\mathbf{PF6}}$ (based on 0.5 mmol of $[Mo(dmbd)_3]$). Yield: 200 mg (0.21 mmol, 42%). Anal. Calcd for $C_{62}H_{64}P_2BMo$: C, 76.15%; H, 6.55%. Found: C, 76.41%; H, 6.53%.

Preparation of [Mo(dmbd)(dppe)] (3). A suspension of 400 mg (0.5 mmol) of $[Mo(dmbd)_2(dppe)](PF_6)$ ($\mathbf{2}^{\mathbf{PF6}}$) in 15 mL of THF was added to sodium amalgam (150 mg Na in 20 g Hg). The mixture was stirred overnight. The brown solution was decanteted, filtred, and reduced under vacuum conditions to 3 mL. After the addition of 8 mL of methanol, the solution was reduced again, and another 8 mL of methanol was added. The orange precipitate was filtered and dried under vacuum conditions. Yield: 180 mg crude product (0.27 mmol, 55%). Recrystallization by layering a benzene solution with *n*-hexane leads to orange crystals. Anal. Calcd for $C_{38}H_{44}P_2Mo$: C, 69.30%; H, 6.68%. Found: C, 69.51%; H, 6.80%.

^{1}H NMR (δ, thf-d^8, 213 K): 7.90−7.06 (m, 20H, Ph), 2.59 (broad m, 2H, CH_2-dppe), 2.60 (broad m, 2H, CH_2-dppe), 1.73 (s, 6H, $-CH_3$), 1.64 (s, 6H, $-CH_3$), 0.58 (s, 2H, *syn*-CH_2, H^2), 0.40 (d, J(P−H) = 21.24 Hz, 2H, *syn*-CH_2, H^4), −1.26 (d, J(H−H) = 6.28 Hz, 2 H, *anti*-CH_2, H^1), −2.64 (dd, J(H−H) = 6.28 Hz, J(P−H) = 10.85 Hz, 2H, *anti*-CH_2, H^3). ^{13}C{^{1}H} NMR(δ, thf-d^8, 213 K): 135−126 (Ph), 91.99 (C^c), 83.64 (C^b), 51.25 (C^d), 36.64 (C^a), 28.86 (dppe-CH_2), 19.40/19.21 ($-CH_3$). ^{31}P{H} NMR (δ,thf-d^8, 213 K, 213 K): 77.01 (2 P, dppe).

Isolation and Characterization of $[MoF_2(dppe)_2](BF_4)$ (4). If fluoride-containing ferrocenium salts, especially $FcBF_4$, were employed in the oxidation of $\mathbf{1}^{\mathbf{dmbd}}$, a small amount of the molybdenum(III) complex $[MoF_2(dppe)_2](BF_4)$ (**4**) could be isolated. Single crystals of **4** were characterized by X-ray structure analysis. This compound has already been obtained as one of the reaction products of $[MoH_4(dppe)_2]$ with HBF_4.[24]

III. RESULTS AND ANALYSIS

A. Vibrational Spectra and Assigments of $[Mo(bd)_3]$ ($\mathbf{1}^{\mathbf{bd}}$). Infrared and Raman spectra of molybdenum butadiene complexes allow one to assess the degree of backbonding from the metal to the ligands. In order to analyze these data, the vibrational spectra of $\mathbf{1}^{\mathbf{bd}}$ have been investigated in detail with the help of DFT. The optimized structure of $\mathbf{1}^{\mathbf{bd}}$ is shown in Figure 1. The MIR regions of the measured and calculated IR

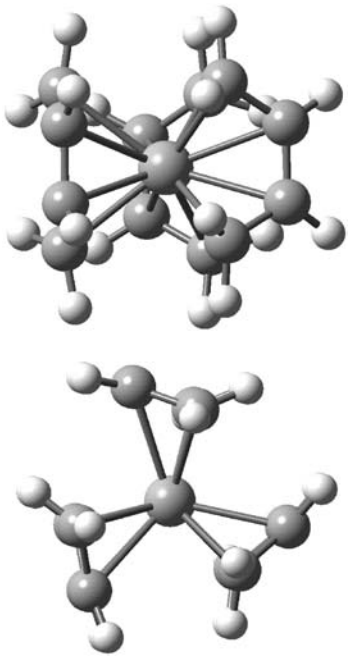

Figure 1. Optimized structure of $[Mo(bd)_3]$ ($\mathbf{1}^{\mathbf{bd}}$).

spectra are shown in Figure 2; corresponding Raman spectra are given in Figure 3. In general, the calculated spectrum is shifted to somewhat higher energy compared to the experiment; the average deviation in vibrational energies is about 2 to 3%. Nevertheless, the relative energies and intensities of the calculated and measured IR and Raman spectra match quite well and enable an unequivocal assignment of the vibrational modes.

The tris(butadiene) complex $\mathbf{1}^{\mathbf{bd}}$ exhibits $3N - 6 = 87$ normal modes. Selected eigenvectors are shown in Figure S1, Supporting Information. In the C_{3h} point group of the complex, the modes transform according to the A′, A″, E′, or E″ irreducible representations. The complex has 18 C−H stretching modes (3 × A′, 3 × A″, 3 × E′, and 3 × E″, **87**−**70** in Table 2). The most intense bands in the Raman spectrum at 3054 cm^{-1} and 2976 cm^{-1} can be assigned to the combination of the antisymmetric CH_2 stretch with the symmetric CHCH stretching mode (**85**, A′, calcd. 3240 cm^{-1}) and the antisymmetric CH_2 stretching mode (**70**, A′,

dx.doi.org/10.1021/ic400145f | Inorg. Chem. 2013, 52, 5931−5942

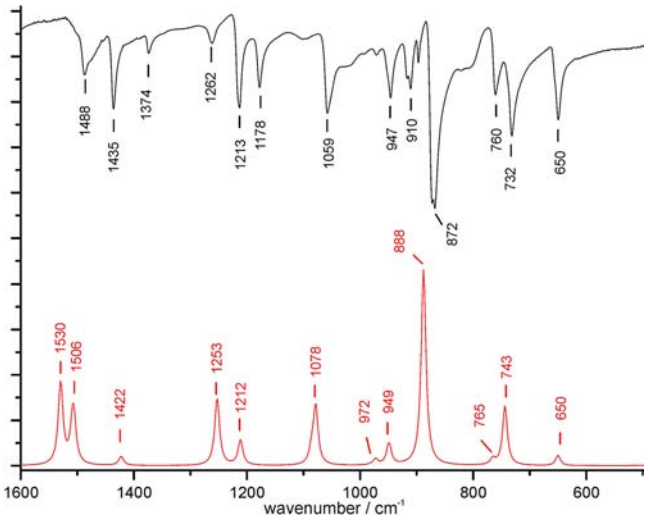

Figure 2. Measured (black) and calculated IR spectra (red) of $[Mo(bd)_3]$ ($\mathbf{1}^{bd}$).

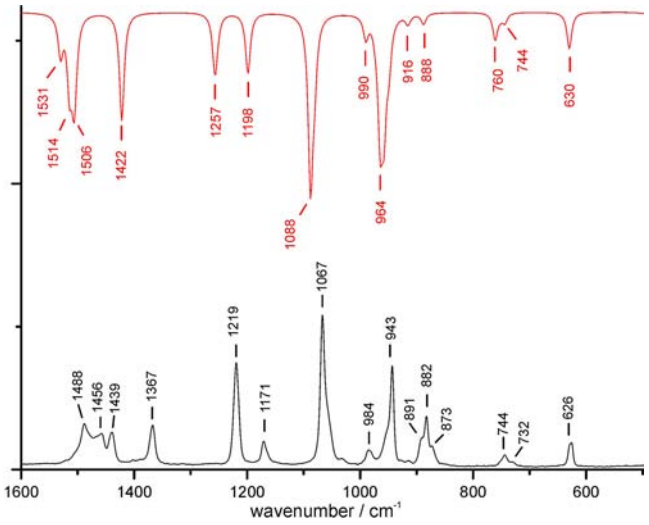

Figure 3. Measured (black) and calculated Raman spectra (red) of $[Mo(bd)_3]$ ($\mathbf{1}^{bd}$).

calcd. 2976 cm^{-1}), respectively. The IR spectrum in the region >2800 cm^{-1} is dominated by two peaks at 3047 cm^{-1} and 2978 cm^{-1}. The vibration at 3047 cm^{-1} corresponds to a combination of an antisymmetric CH_2 vibration with an antisymmetric CHCH vibration (**84**, A″, calcd. 3234 cm^{-1}), whereas the band at 2978 cm^{-1} is due to a degenerate symmetric vibration of the terminal CH_2 groups (**72**/**71**, E′, calcd. 3132 cm^{-1}).

At lower frequencies than the C−H stretching vibrations, the modes with C−C stretching and C−H deformation contributions are located. The vibration at highest energy in this region is observed at 1488 cm^{-1} in the Raman spectrum (**69**, calcd. 1531 cm^{-1}; Figure 3). It can be assigned to the A′ vibration (**69**) that is dominated by the stretching motion of the *central* C−C bond. Additionally, deformations of the CH_2 and CH groups contribute to this vibration. The corresponding vibration mode in E′ symmetry is associated with a band at 1488 cm^{-1} in the IR spectrum (**68**/**67**, calcd. 1530 cm^{-1}). The stretching vibrations of the *terminal* C−C bonds mixed with C−H deformations in E″ symmetry cause a band at 1456 cm^{-1} in the Raman spectrum (**66**/**65**, calcd. 1514 cm^{-1}). The corresponding A″ mode **64** which is calculated at 1509 cm^{-1}

Table 2. Selected Frequencies of $[Mo(bd)_3]$ ($\mathbf{1}^{bd}$)

mode	no.	calculated frequency/ cm^{-1}	experimental frequency/ cm^{-1}	symmetry in C_{3h}
$\nu(CC)_{central} + \delta(CH2) + \delta(CHCH) + \nu(CC)_{sym,terminal}$	69	1531	1488 (RA)	A′
$\nu(CC)_{central} + \delta(CH_2) + \delta(CHCH) + \nu(CC)_{sym,terminal}$	68/67	1530	1488 (IR)	E′
$\nu(CC)_{asym,terminal} + \delta(CH_2) + \rho_r(CHCH)$	66/65	1514	1456 (RA)	E″
$\nu(CC)_{asym,terminal} + \delta(CH_2) + \rho_r(CHCH)$	64	1509		A″
$\nu(CC)_{central} + \delta(CH_2) + \delta(CHCH)$	63/62	1506	1439 (RA), 1435 (IR)	E′
$\nu(CC)_{central} + \delta(CH_2) + \delta(CHCH)$	61	1503		A′
$\delta(CH_2) + \rho_r(CHCH) + \delta(CC)_{asym,terminal}$	60	1422	1374 (IR)	A″
$\delta(CH_2) + \rho_r(CHCH) + \nu(CC)_{asym,terminal}$	59/58	1422	1367 (RA)	E″
$\rho_r(CHCH) + \delta(CH_2) + \nu(CC)_{sym,terminal}$	57	1257	1219 (RA)	A′
$\rho_r(CHCH) + \delta(CH_2) + \nu(CC)_{sym,terminal}$	56/55	1253	1213 (IR)	E′
$\rho_r(CHCH) + \delta(CH_2) + \delta(CCC)_{asym}$	54	1212	1178 (IR)	A″
$\rho_r(CHCH) + \delta(CH_2) + \delta(CCC)_{asym}$	53/52	1198	1171 (RA)	E″
$\delta(CHCH) + \delta(CH_2) + \delta(CCC)_{sym}$	51	1088	1067 (RA)	A′
$\delta(CHCH) + \delta(CH_2) + \delta(CCC)_{sym}$	50/49	1086		E′
$\rho_r(CHCH) + \delta(CH_2) + \nu(CC)_{asym,terminal}$	48/47	1080		E″
$\rho_r(CHCH) + \delta(CH_2) + \nu(CC)_{asym,terminal}$	46	1078	1059 (IR)	A″
$\rho_t(CHCH)_{sym} + \rho_w(CH_2)_{sym}$	45/44	990	984 (RA)	E″
$\rho_t(CHCH)_{sym} + \rho_w(CH_2)_{sym}$	43	980		A″
$\rho_w(CH_2) + \delta(CHCH) + \nu(CC)_{sym,terminal} + \nu(CC)_{sym,central}$	42/41	972	947 (IR)	E′
$\rho_w(CH_2) + \delta(CHCH) + \nu(CC)_{sym,terminal} + \nu(CC)_{sym,central}$	40	964	943 (RA)	A′
$\rho_w(CH_2)_{asym} + \rho_w(CHCH)$	39	958		A′
$\rho_w(CH_2)_{asym} + \rho_w(CHCH)$	38/37	949	910 (IR)	E′
$\rho_w(CH_2)_{asym} + \rho_t(CHCH)$	36	948		A″
$\rho_w(CH_2)_{asym} + \rho_t(CHCH)$	35/34	916	882 (RA)	E″
$\rho_w(CHCH)_{sym} + \rho_w(CH_2)_{sym}$	33	912		A′
$\rho_w(CHCH)_{sym} + \rho_w(CH_2)_{sym}$	32/31	888	872 (IR, RA)	E′
$\rho_t(CH_2)_{sym}$	30	765	760 (IR)	A″
$\rho_t(CH_2) + \rho_w(CHCH)_{sym}$	29	760	732 (RA)	A′
$\rho_t(CH_2) + \delta(CCC)$	28/27	751		E″
$\rho_t(CH_2) + \rho_w(CHCH) + \delta(CCC)$	25/26	743	732 (IR, RA)	E′
$\delta(CCC)$	24	650	650 (IR)	E″
$\delta(CCC)$	23/22	630	626 (RA)	E″

dx.doi.org/10.1021/ic400145f | Inorg. Chem. 2013, 52, 5931−5942

could neither be identified in the IR nor in the Raman spectrum. The E′ vibrations **63** and **62** are dominated by the stretching vibration of the central C−C bond and the deformation of the terminal CH_2 group. They give rise to a band in the Raman spectrum at 1439 cm^{-1} and in the IR spectrum at 1435 cm^{-1}, respectively (calcd. 1506 cm^{-1}). The calculations show that the corresponding A′ vibration (**61**, calcd. 1503 cm^{-1}) has no intensity in the IR and only weak intensity in the Raman spectrum. Therefore, it could not be identified in the experimental spectra.

The bands in the IR spectrum at 1374 cm^{-1} (calcd. 1422 cm^{-1}) and 1367 cm^{-1} (calcd. 1422 cm^{-1}) can be assigned the A″ vibration **60** and the E″ vibrations **59** and **58**, respectively. They represent combinations of deformations of the terminal CH_2 and both central CH groups. The vibrations following to lower energy are combinations of these deformations as well. Vibration **57** in A′ symmetry gives rise to an intense band at 1219 cm^{-1} (calcd. 1257 cm^{-1}). The vibrations in E′ symmetry **56**/**55** cause a band in the IR spectrum at 1213 cm^{-1} (calcd. 1253 cm^{-1}). At lower wavenumbers, the combinations of C−C deformations of the butadiene backbone can be found. Specifically, the bands at 1178 cm^{-1} (**54**, A″, calcd. 1212 cm^{-1}) in the IR and at 1171 cm^{-1} (**53**/**52**, E″, calcd. 1198 cm^{-1}) in the Raman are due to combinations of δ(CCC) and CH deformations. While these vibrations are antisymmetric with respect to the mirror plane of the complex, the symmetric modes cause an intense band in the Raman spectrum at 1067 cm^{-1} (**51**, A′, calcd. 1088 cm^{-1}). The calculations show that the corresponding E′ (**50**/**49**, calcd. 1086 cm^{-1}) has low intensity and can therefore not be identified in the experimental spectra.

The CH out-of-plane vibrations can be found in the region below 1000 cm^{-1}. The most intense peaks are at 943 cm^{-1} in the Raman and at 872 cm^{-1} in the IR spectrum. The band at 943 cm^{-1} can be assigned to the A′ mode dominated by a wagging vibration of the terminal CH_2 group (**40**, calcd. 963 cm^{-1}). The band at 872 cm^{-1} has E′ symmetry and is caused by out of plane CH vibrations (**32**/**31**, calcd. 888 cm^{-1}). It can also be identified in the Raman spectrum, giving rise to a weak peak at 873 cm^{-1}. The calculation shows that the bands in the lower region are due to further CH out-of-plane vibrations and CC torsion modes. Vibrations with metal ligand stretching character, finally, can be found below 400 cm^{-1}.

The vibrational properties of [Mo(dmbd)$_3$] (**1**^{dmbd}) were evaluated in a similar way. The optimized structure of **1**^{dmbd} as well as the measured and calculated spectra are given in the Supporting Information, Figures S2−S4. However, due to the strong coupling of the vibrations of the diene unit with the methyl groups at the central carbon atoms, the assignment of the individual modes is less clear-cut.

The identification of the bands containing C−C stretching modes is useful for the interpretation of the bonding situation in the coordinated butadiene units. The highest-energetic C−C vibration of free *trans*-1,3-butadiene is the ν_4 mode at 1644 cm^{-1} containing C═C stretching motions of the two double bonds.[25] The importance of backbonding is indicated by the fact that the corresponding modes appear at much lower frequencies in the complex (Table 2). The vibrational analysis further shows that none of the C−C bonds can be described as a pure double or single bond but that these vibrations are in fact strongly mixed.

B. Normal Coordinate Analysis of [Mo(bd)$_3$] (1^{bd}). In order to obtain further insight into the coordination of the butadiene ligands to molybdenum centers, the central and terminal C−C force constants of the bd ligands in the complex [Mo(bd)$_3$] (**1**^{bd}) were calculated. To this end, the set of Cartesian force constants derived from the DFT vibrational analysis was converted into a set of internal force constants by the program REDONG.[23] A force field was employed which describes each coordinated bd ligand in terms of a central and a terminal C−C force constant, a Mo−C_{int} metal−carbon force constant, and six C−H force constants (Scheme 1). Around each central and each terminal C atom of a coordinated bd ligand, six (respectively three) bending force constants are defined. Each terminal C−C bond is associated with a torsion. In order to describe the relative motions of the three bd ligands around the Mo(0) center, six C_{out}−Mo−C_{out} bends and six torsions around the Mo−C_{out} bonds are introduced. The resulting force field exhibits 18 redundancies.

Scheme 1. Force Field Employed for the Normal Coordinate Analysis of [Mo(bd)$_3$] (1^{bd})[a]

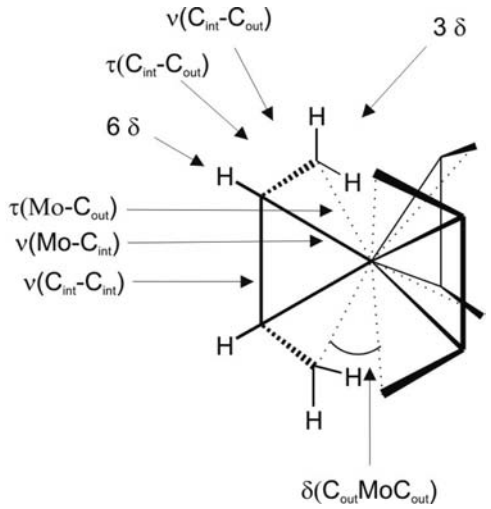

[a]For clarity, H atoms are omitted on two of the three bd ligands.

On the basis of the Cartesian force constants calculated by DFT by the described procedure are given internal force constants f of 4.79 mdyn/Å for the central and 3.97 mdyn/Å for the terminal C−C bonds. Uncoordinated (*trans*-) butadiene, in contrast, exhibits an $f_{central}$ of 5.20 mdyn/Å and an $f_{terminal}$ of 8.87 mdyn/Å.[25] Upon coordination to the Mo(0) center, both C−C force constants of free butadiene thus are lowered, but $f_{terminal}$ about 7 times more (−55%) than $f_{central}$ (−8%). The large decrease of $f_{terminal}$ and the weak decrease of $f_{central}$ are due to the fact that metal → ligand backbonding involves the ψ^3 orbital of butadiene, which is antibonding with respect to the terminal C−C bonds and bonding with respect to the central C−C bond (see below).

C. Synthesis and Reactivities of the Cationic Molybdenum Complexes 2. The 17-electron complex [Mo(dmbd)(dppe)](BPh$_4$) (**2**^{BPh}) was synthesized by one-electron oxidation of [Mo(dmbd)$_3$] (**1**^{dmbd}) in the presence of 1,2-bis(diphenylphosphino)ethane (dppe) in thf. Ferrocinium salts (FcX, X = BF_4^-, PF_6^-, BPh_4^-) were used as oxidizing reagents. All compounds could be isolated in good yields as air stable green powders. The complexes are well soluble in CH_2Cl_2, $CHCl_3$, and nitriles, whereas they are insoluble in nonpolar solvents like toluene and hexane and in alcohols. If fluoride-containing ferrocenium salts, especially $FcBF_4$, are employed, sometimes small amounts of impurities appear that

dx.doi.org/10.1021/ic400145f | Inorg. Chem. 2013, 52, 5931−5942

can be separated by crystallization. Under these conditions, a few crystals of the complex $[MoF_2(dppe)_2](BF_4)$ (**4**) were isolated and characterized by X-ray structure analysis. This compound is already known as one of the reaction products of $[MoH_4(dppe)_2]$ with HBF_4.[24] The addition of $FcBF_4$ to $\mathbf{2}^{BF4}$, however, did not lead to the formation of **4**.

By reduction of **2** with sodium amalgam in thf overnight, the molybdenum complex $[Mo(dmbd)_2(dppe)]$ (**3**) was synthesized. The orange compound is unstable under aerobic conditions in solution; i.e., it decomposes under precipitation of a green compound which could be characterized by X-ray crystallography and identified as the 17-electron complex $[Mo(dmbd)_2(dppe)]_2(Mo_2O_7)$ (data not shown).

Importantly, **3** could not be obtained by ligand exchange of $[Mo(dmbd)_3]$ ($\mathbf{1}^{dmbd}$) under thermal conditions, even by refluxing $[Mo(dmbd)_3]$ with dppe in acetonitrile or toluene. The fact that $\mathbf{1}^{dmbd}$ is inert toward substitution and the occurrence of the butadiene-free complex $[MoF_2(dppe)_2](BF_4)$ (**4**) in the reaction product suggest the following reaction mechanism (Scheme 2): The unreactive complex $[Mo(dmbd)_3]$ is oxidized first to a $[Mo(dmbd)_3]^+$ cation. In this oxidation state, one of the weaker bound diene ligands can be substituted by a bidentate dppe, forming the stable $17e^-$ complex $[Mo(dmbd)_2(dppe)]^+$ (**2**). As a side reaction, also the substitution of one dmbd against fluoride can occur. This fluoride-containing intermediate can further be oxidized and fluorine-substituted, leading to the complex $[MoF_2(dppe)_2]^+$ (**4**).

The molybdenum complex $[Mo(bd)_3]$ ($\mathbf{1}^{bd}$) exhibits a different reactivity as compared to its methylated counterpart. Use of $FcBF_4$ or $FcPF_6$ as oxidants leads to an undefined mixture of products with small fractions of a green compound. This observation suggests that the nonmethylated complex has a much higher reactivity toward fluoride ions, leading to different fluorinated compounds as main products. Using the halide-free oxidizing reagent $FcBPh_4$, on the other hand, was found to lead to a green oily reaction product which can be isolated as a foamy solid after drying under vacuum conditions. No further characterization of this compound could be achieved. Exchange of the anion might possibly lead to a crystalline product.

The differences in reactivity between $\mathbf{1}^{bd}$ and $\mathbf{1}^{dmbd}$ indicate that steric shielding imposed by the methyl groups must have a large influence. Especially the 17-electron trisdiene species seems to be much more reactive toward fluoride substitution for the bd as compared to dmbd intermediate.

D. X-Ray Structure Analysis of $\mathbf{2}^{BPh4}$, 3, and 4. Crystalline substances of **2** were isolated by diffusion of diethylether into an acetonitrile solution. The compounds $\mathbf{2}^{PF6}$ and $\mathbf{2}^{BF4}$ gave no crystals suitable for X-ray diffraction. $\mathbf{2}^{BPh4}$ crystallizes in the triclinic space group $P\bar{1}$ with two complexes and two tetraphenylborate counterions per unit cell (cf Table 1). The complex is C_2-symmetric with the 2-fold axis bisecting the angle P1−Mo1−P2. The structure is shown in Figure 4. Both *cis*-2,3-dimethylbutadiene ligands are bound in an η^4 mode to the molybdenum center with a basically planar butadiene skeleton. The ligands are not coordinated in an eclipsed fashion but are twisted by an angle of 52.9° (the twist angle is defined as the angle between the projections on the P−Mo−P plane of the vectors from the centers of the butadiene ligands to the Mo center). The dppe ligand exhibits a bite angle of 77.68(1)°. The P1 atom of the dppe ligand is bound in *trans* position to C3 and C4; P2 is located in *trans* position to C13 and C14.

Scheme 2. Reaction Scheme for the Oxidative Substitution of Tris(2,3-dimethylbutadiene)molybdenum, $\mathbf{1}^{dmbd}$

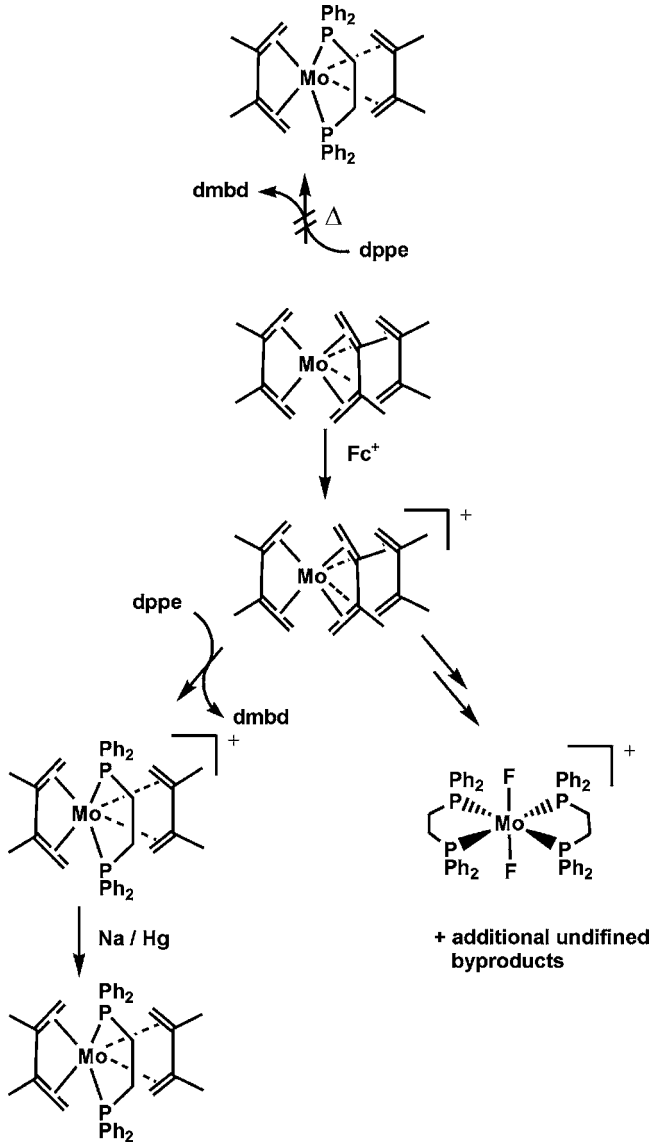

The C−C bonds of the butadiene ligands show an equalization of the bond lengths due to extensive backbonding into the π^* orbitals of the diene units. In contrast to the parent compound $[Mo(dmbd)_3]$ ($\mathbf{1}^{dmbd}$), where the central C−C bond (1.396(3) Å) is shorter than the terminal bonds (1.439(3) Å), the C−C bonds in $\mathbf{2}^{BPh4}$ have similar values ranging from 1.418(5) Å to 1.433(5) Å.[26,27] Due to this strong backbonding effect, the terminal CH_2 groups of the 2,3-dimethylbutadiene ligands are not planar anymore, indicating a change from sp^2 to sp^3 character (see below). The distances from the metal to the terminal C atoms have comparable values for both dmbd ligands, ranging from 2.272(4) Å to 2.289(4) Å. The distances from the metal to the central C atoms C2 (2.344(3) Å) and C12 (2.344(4) Å) are slightly shorter as compared to C3 (2.372(4) Å) and C13 (2.367(4) Å), which approximately are in *trans* position to the phosphorus atom P2. Crystals of a corresponding 17-electron complex were isolated by the diffusion of diethylether into an acetonitrile solution of

dx.doi.org/10.1021/ic400145f | Inorg. Chem. 2013, 52, 5931−5942

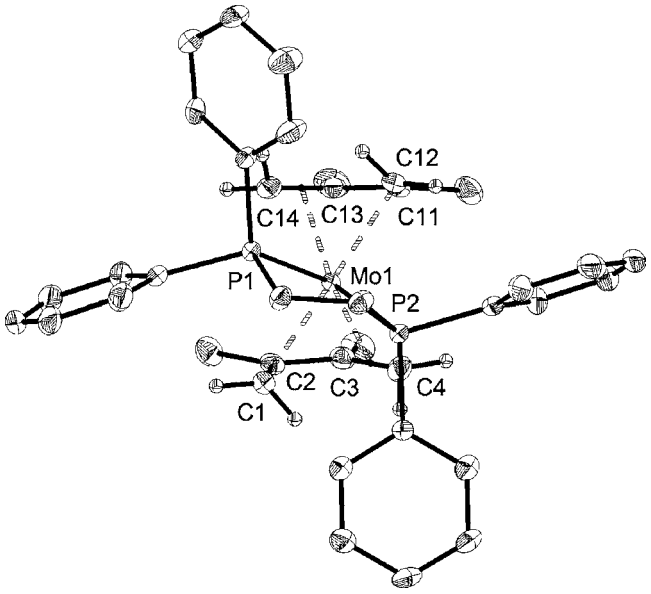

Figure 4. Crystal structure of $[Mo(dmbd)_2(dppe)](BPh_4)$ ($\mathbf{2}^{BPh4}$; 50% ellipsoids, hydrogen atoms omitted). Selected bond lengths (Å) and angles (deg): Mo(1)−C(1) 2.272(4), Mo(1)−C(14) 2.282(3), Mo(1)−C(11) 2.288(4), Mo(1)−C(4) 2.289(4), Mo(1)−C(12) 2.344(4), Mo(1)−C(2) 2.344(3), Mo(1)−C(13) 2.367(4), Mo(1)−C(3) 2.371(4), Mo(1)−P(2) 2.5395(10), Mo(1)−P(1) 2.5556(10), C(1)−C(2) 1.423(5), C(2)−C(3) 1.423(5), C(3)−C(4) 1.433(5), C(11)−C(12) 1.425(6), C(12)−C(13) 1.418(5), C(13)−C(14) 1.429(5), C(1)−C(2)−C(3) 117.4(3), C(2)−C(3)−C(4) 117.9(4), P(2)−Mo(1)−P(1) 77.68(3), C(1)−Mo(1)−C(4) 74.12(14).

the decomposition product of $[Mo(dmbd)_2(dppe)]$ (**3**). By X-ray crystallography, these crystals were identified as $[Mo(dmbd)_2(dppe)]_2(Mo_2O_7)\cdot 2NCCH_3$ (data not shown).

Single crystals of the corresponding 18-electron complex $[Mo(dppe)(dmbd)_2]$ (**3**) suitable for X-ray diffraction could be isolated by layering a benzene solution with *n*-hexane. The compound crystallizes in the monoclinic space group $P2_1/n$ with four molecules per unit cell. The structure of the complex is given in Figure 5; crystallographic data are collected in Table 1.

With two η^4 bonded 2,3-dimethylbutadienes and one bidentate dppe ligand, the complex has a similar C_2-symmetrical structure to its 17-electron counterpart. In comparison to the cationic complex, the twist of the diene ligands has increased in the neutral complex to 81.44°. Another structural difference to the cationic complex is the larger bite angle of the dppe ligand (81.17(1)°). Interestingly the oxidation state of the metal center has no significant influence on the C−C bond lengths of the diene ligands. As in the neutral trisbutadiene complex **1** and in the cationic complex $\mathbf{2}^{PPh4}$, an equalization of the C−C bond lengths is observed for **3**. In contrast to $\mathbf{1}^{dmbd}$, where the central C−C bond lengths are slightly shorter than the terminal ones (*vide supra*), the C−C bond lengths in **2** have comparable values ranging from 1.420(3) Å to 1.440(5) Å. The molybdenum−carbon distances for the terminal C atoms have similar values ranging from 2.271(2) Å (Mo−C(14)) to 2.291(6) Å (Mo−C(11)). Like in compound **2**, the distances from molybdenum to the central carbon atoms approximately in *trans* position to the P atoms, C3 (2.323(5) Å) and C13 (2.307(3) Å), are slightly longer as compared to Mo−C2 (2.285(4) Å) and Mo−C12 (2.283(9) Å). A similar bonding situation has also been determined for the complex $[Mo(bd)_2(PMe_3)_2]$.[14]

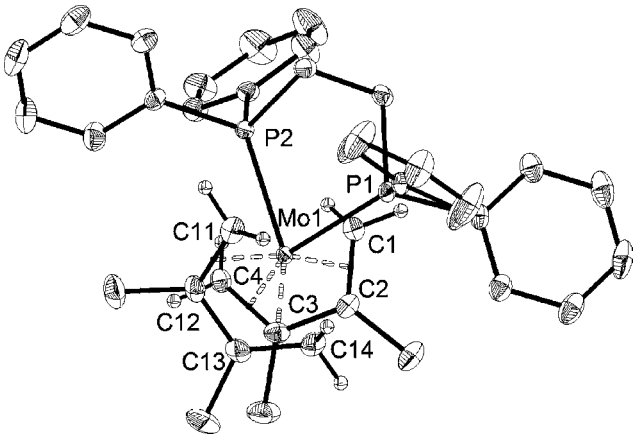

Figure 5. Crystal structure of $[Mo(dmbd)_2(dppe)]$ (**3**; 50% ellipsoids, hydrogen atoms omitted). Selected bond lengths (Å) and angles (deg): Mo(1)−C(14) 2.271(2), Mo(1)−C(12) 2.283(9), Mo(1)−C(2) 2.285(4), Mo(1)−C(1) 2.287(9), Mo(1)−C(4) 2.289(3), Mo(1)−C(11) 2.291(6), Mo(1)−C(13) 2.307(3), Mo(1)−C(3) 2.323(5), Mo(1)−P(1) 2.466(3), Mo(1)−P(2) 2.476(6), C(1)−C(2) 1.440(5), C(2)−C(3) 1.420(3), C(3)−C(4) 1.428(3), C(11)−C(12) 1.432(5), C(12)−C(13) 1.420(3), C(13)−C(14) 1.435(3), C(3)−C(2)−C(1) 114.63(16), C(2)−C(3)−C(4) 116.92(15), P(1)−Mo(1)−P(2) 81.17(1), C(2)−Mo(1)−C(1) 36.70(6).

Single crystals of the byproduct $[MoF_2(dppe)_2](BF_4)$ (**4**) could be isolated by diffusion of diethylether into an acetonitrile solution of the reaction product of $[Mo(dmbd)(dppe)](BF_4)$. The complex crystallizes in the monoclinic space group *Cc* with four complexes and four BF_4^- counterions per unit cell (Table 1). The Mo center is octahedrally coordinated with the two diphos ligands in the equatorial plane and two F^- ligands in axial positions (Figure 6).

The Mo−P distances have values from 2.5260(6) Å to 2.5549(6) Å. The metal flouride distances are 1.8605(16) Å and 1.8732(17) Å. The bite angles of the dppe ligand are 79.29(2) Å; the F−Mo−F angle is 178.33(8) Å.

E. Spectroscopic and Magnetic Properties of Compounds 2 and 3. The 17-electron complex $\mathbf{2}^{PF6}$ gives rise to a heavily split signal in the room temperature EPR spectrum at g = 2.0146 (Figure 7). The complicated signal structure is caused by hyperfine coupling of the unpaired spin with the two phosphines and the four different CH_2 protons; the I = 5/2 isotopes ^{95}Mo and ^{97}Mo cause an additional splitting. Magnetic measurements of $\mathbf{2}^{PF6}$ indicate a paramagnetic behavior with a magnetic moment of 1.73 μ_B per formula unit (Figure S5, Supporting Information). Both data sets thus are consistent with the presence of one unpaired electron.

The corresponding neutral complex **3** is, of course, diamagnetic but exhibits a temperature-dependent ^{1}H NMR spectrum revealing significant structural dynamics in solution.

The denominations of the C and H atoms of **3** are given in Figure 8. Figure 9 shows the signals of the *endo*-CH_2 protons H^1 and H^3 in thf-d^8 solution (*endo* hydrogens are placed away from the molybdenum, cf. Figure 8). Due to the C_2 symmetry of the complex, these protons give rise to two resonances at −1.20 ppm and −2.46 ppm; at room temperature, these resonances are broad. Cooling the solution to below 240 K leads to better resolved signals located at −1.26 ppm (broad d, H^1, J(H−H) = 6.2 Hz) and −2.65 ppm (broad dd, H^3, J(H−H)

dx.doi.org/10.1021/ic400145f | Inorg. Chem. 2013, 52, 5931−5942

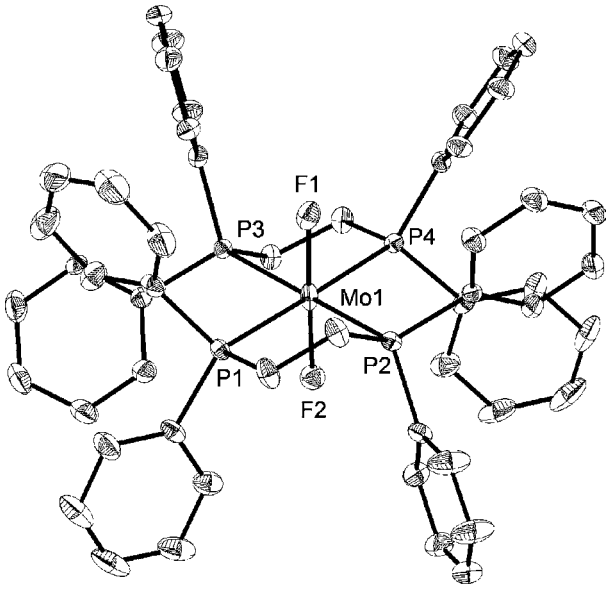

Figure 6. Crystal structure of $[MoF_2(dppe)_2](BF_4)$ (**4**; 50% ellipsoids, hydrogen atoms omitted). Selected bond lengths (Å) and angles (deg): Mo(1)−F(2) 1.8605(16), Mo(1)−F(1) 1.8732(17), Mo(1)−P(1) 2.5518(6), Mo(1)−P(2) 2.5418(6), F(2)−Mo(1)−F(1) 178.33(8), P(2)−Mo(1)−P(1) 79.29(2), P(3)−Mo(1)−P(4) 79.29(2).

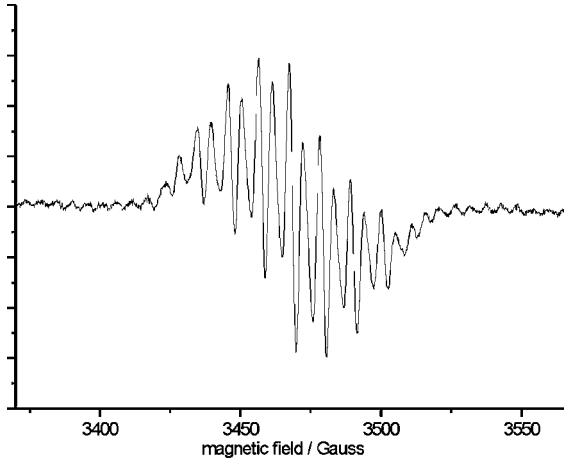

Figure 7. EPR spectrum of $[Mo(dmbd)_2(dppe)](PF_6)$ ($\mathbf{2}^{PF6}$).

= 6.2 Hz, J(P−H) = 10.4 Hz; line width ∼5 Hz). The *exo*-CH_2 protons H^2 and H^4, on the other hand, give two resonances at 0.40 ppm (broad d, H^4, J(P−H) = 21.2 Hz) and 0.58 ppm (broad s, H^2), and the CH_3 groups (H^5, H^6) lead to two signals at 1.60 ppm and 1.73 ppm, respectively (all values at room temperature). The dppe ligand, finally, causes two broad multiplets for the CH_2 protons (H^7, H^8, 2.66 ppm, 3.49 ppm) and multiplets ranging from 7.05 ppm to 7.93 ppm for the phenyl protons.

The temperature dependence of the ^{1}H NMR spectrum of **3** is remarkable in view of the fact that the corresponding trimethylphosphine butadiene complex $[Mo(bd)_2(PMe_3)_2]$ does not show comparable behavior.[14] It can be assumed that the line broadening at 300 K is caused by a conformational change of the complex with the two diene ligands exchanging their position, which is accompanied by a twist of the dppe ligand. At lower temperatures, the structure becomes more

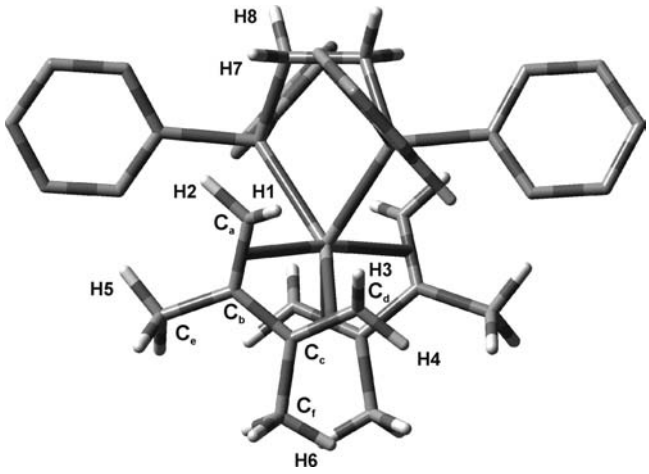

Figure 8. Assignment of C and H atoms of **3** for the analysis of ^{1}H and ^{13}C NMR spectra.

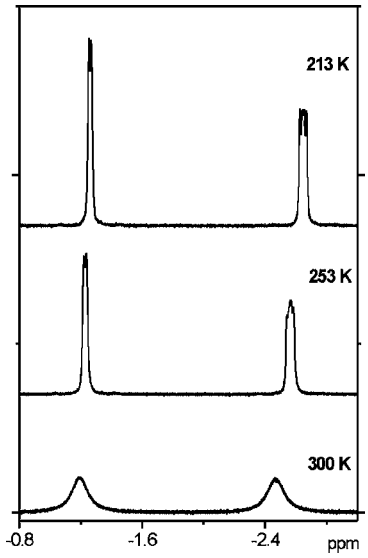

Figure 9. Temperature-dependent ^{1}H NMR spectrum of **3** (*endo*-CH_2 protons).

static. This is also reflected by the ^{31}P NMR spectra; i.e., upon cooling from 300 to 213 K, the line width of the resonance at 76.9 ppm decreases from 50 to 20 Hz.

As shown previously, the ^1J(C−H) coupling constants of butadiene and dimethylbutadiene complexes can be correlated with the hybridization at the corresponding C atoms, providing important information with respect to the degree of back-bonding in these compounds.[28] For the $^1J(H^1-C_a)$ coupling constant of compound **3** (cf Figure 8), a value of 149 Hz is obtained. Importantly, this value is very similar to those found for the homoleptic complexes $[Mo(bd)_3]$ and $[Mo(dmbd)_3]$ (cf Table 3; representative sections of NMR spectra are shown in Figure S6, Suppurting Information) as well as $[W(bd)_3]$ and $[W(dmbd)_3]$.[29] This indicates that the amount of backbonding from the metal center to the butadiene ligands in **3** is very similar to that of the neutral Mo and W tris(diene) counterparts. Using Newton's empirical relation, a coupling constant of 150 Hz can be correlated with 29.54% s character and, correspondingly, a hybridization of $sp^{2.385}$,[30] indicative of a significant charge transfer from the Mo center to the double bonds of the butadiene ligands.

dx.doi.org/10.1021/ic400145f | *Inorg. Chem.* 2013, 52, 5931−5942

Table 3. ^1J(C−H) Coupling Constants for the Terminal C Atoms of Butadiene and Dimethyl-Butadiene Ligands Coordinated to Mo and W Complexes (at Room Temperature; n.r. = Not Resolved; Shifts in Parentheses; for 3 Parameters at 213 K Are Given)

compound	*endo* ^1J(C−H)	*exo* ^1J(C−H)	ref.
$[Mo(bd)_3]$ ($\mathbf{1}^{bd}$)	150 Hz (0.48 ppm)	154 Hz (1.6 ppm)	this work
$[W(bd)_3]$	151 Hz (0.35 ppm)	151 Hz (1.42 ppm)	Benn et al.[29]
$[Mo(dmbd)_3]$ ($\mathbf{1}^{dmbd}$)	152 Hz (−0.27 ppm)	*n.r.* (1.46 ppm)	this work
$[W(dmbd)_3]$	147 Hz (−0.33 ppm)	147 Hz (1.13 ppm)	Benn et al.[29]
$[Mo(dmbd)_2(dppe)]$ (**3**)	149 Hz (−1.26 ppm)	*n.r.* (0.40 ppm)	this work
	n.r. (−2.65 ppm)	*n.r.* (0.58 ppm)	

As shown for the parent compound $[Mo(bd)_3]$ ($\mathbf{1}^{bd}$; *vide supra*), important information on the bonding situation of the butadiene ligands coordinated to molybdenum centers is also provided by vibrational spectroscopy. The Raman spectra of compounds **2** and **3** (Figure 10) exhibit almost the same signals

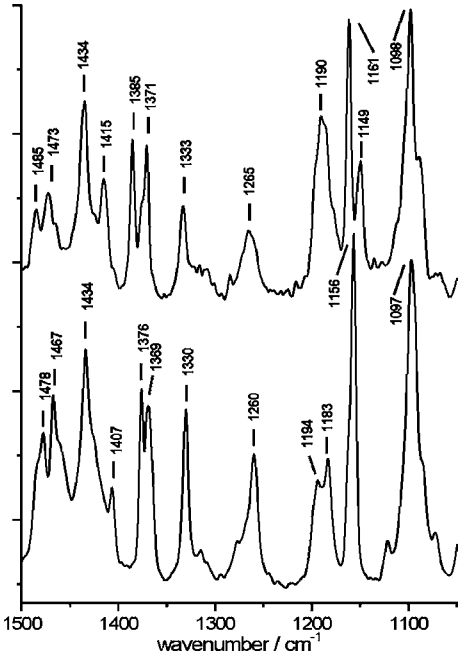

Figure 10. Raman spectrum of $[Mo(dmbd)(dppe)](BPh_4)$ ($\mathbf{2}^{BPh4}$, top) and $[Mo(dmbd)(dppe)]$ (**3**, bottom).

as $\mathbf{1}^{bd}$ and $\mathbf{1}^{dmbd}$ in the region from 1500 cm^{-1} to 1000 cm^{-1}, which is characteristic for the C−H-deformation and C−C-stretching vibrations; the IR spectra of compounds $\mathbf{2}^{BPh4}$ and **3** are given in the Supporting Information, Figure S6. A detailed vibrational assignment on the basis of DFT calculations, as performed for $\mathbf{1}^{bd}$, is difficult for these compounds due to the strong mixing of the C−C stretching vibrations with the CH_3 deformations. Nevertheless, the Raman spectra clearly indicate that the bonding of the diene ligands does not change upon one-electron oxidation of the metal center in **3**, leading to **2**. This is compatible with the C−C bond lengths determined from the X-ray structures. Furthermore, vibrational spectroscopy reveals that the bonding of the diene ligands is very similar in the homoleptic complexes **1** and the heteroleptic complex **3**, which is also compatible with the C−C bond lengths and the observed ^1J(C−H) coupling constants.

F. Electrochemical Properties. The cyclic voltammogram of compound $\mathbf{2}^{PF6}$ (Figure 11) shows a quasi-reversible one-

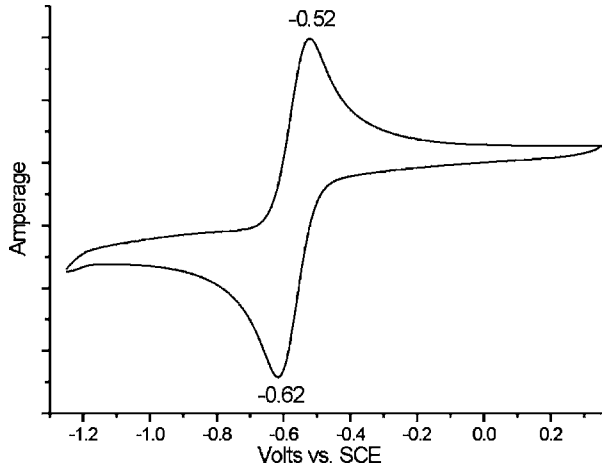

Figure 11. Cyclic voltammogram of $\mathbf{2}^{PF6}$.

electron redox wave at −0.57 V vs SCE which can be assigned to the Mo(I) ↔ Mo(0) redox process. Furthermore, four additional irreversible redox processes could be observed at 1.00, 1.21, and 1.49 V vs SCE, which may be caused by the oxidation to higher oxidation states of the molybdenum center. The difference pulse voltammogram of $\mathbf{2}^{PF6}$ (Figure S7, Supporting Information) shows two more signals at −1.22 V and −1.64 V which appear after running several cycles from −2 V to +2 V. After applying a constant voltage of 2 V for 5 min, the signals disappear. Therefore, they can be assigned to decomposition products on the electrode surface.

G. Electronic Structures of $[Mo(bd)_3]$ ($\mathbf{1}^{bd}$), $[Mo(dmbd)_2(dppe)]^+$ (2), and $[Mo(dmbd)_2(dppe)]$ (3). Further insight into the electronic structures of the heteroleptic Mo(I) and Mo(0) complexes **2** and **3** is provided by DFT, allowing a comparison with the electronic structures of the parent homoleptic molybdenum tris(butadiene) compounds. The optimized structure of $\mathbf{1}^{bd}$ is shown in Figure 1 (*vide supra*). The electronic structure of this complex has been treated before.[2] Table 4 collects structural parameters given in ref 2 in comparison to those calculated in the present study and those determined experimentally; no major differences are observed.

Table 4. Selected Bond Lengths of the Optimized Structure of $[Mo(bd)_3]$ ($\mathbf{1}^{bd}$)

	B3LYP/LANL2DZ	B3LYP[2]	BP86[2]	exptl.[2]
$Mo-C_{terminal}$	2.308	2.302	2.294	2.284/2.273
$Mo-C_{central}$	2.397	2.367	2.360	2.325/2.330
$C_{terminal}-C_{central}$	1.442	1.427	1.434	1.414
$C_{central}-C_{central}$	1.414	1.401	1.408	1.403/1.388

Optimized structures of **2** and **3** are given in the Supporting Information, Figure S8. In agreement with the crystal structures, they show a twisting of the butadiene ligands. In the cationic complex **2**, a twist angle (*vide supra*, C) of 56.55° is calculated (crystal structure 52.9°); the neutral molybdenum complex **3** shows a corresponding angle of 83.00° (crystal structure 81.44°). The trends of the dppe bite angle are

dx.doi.org/10.1021/ic400145f | Inorg. Chem. 2013, 52, 5931−5942

correctly reproduced as well; i.e., the calculated angle for **2** is 77.1° (crystal structure: 77.68(1)°), and the calculated value for **3** is 80.6° (crystal structure: 81.17(1)°). Selected bond lengths and angles of the optimized structures are collected in Table 5.

Table 5. Selected Structural and Calculated Parameters of 2 and 3

	$[Mo(dmbd)_2(dppe)]^+$ (**2**)		$[Mo(dmbd)_2(dppe)]$ (**3**)	
bond lengths/Å, bond angles/deg	exptl.	calcd.	exptl.	calcd.
Mo(1)−C(1)	2.272(4)	2.31	2.287(9)	2.31
Mo(1)−C(2)	2.344(3)	2.41	2.285(4)	2.34
Mo(1)−P(1)	2.5556(10)	2.68	2.466(3)	2.59
P(2)−Mo(1)−P(1)	77.68(3)	77.09	81.17(1)	80.58
C(1)−C(2)	1.423(5)	1.44	1.440(5)	1.45
C(2)−C(3)	1.423(5)	1.44	1.423(5)	1.44

The MO scheme of the neutral molybdenum complex **3** is shown in Figure 12. The HOMO **148** is the d_{z^2} orbital with almost metal−ligand nonbonding character. The HOMO−1 **147** and HOMO−2 **146** are the bonding combinations of the $d_{x^2-y^2}$ and the d_{xz} metal orbitals with the ψ^3 orbitals of the butadiene ligands that form the LUMO in the free ligands (cf. Figure 12). MOs **147** and **146** thus represent the metal−butadiene backbonding interaction in **3**.

Due to the fact that the ψ^3 orbitals are antibonding with respect to the terminal C−C bond and bonding with respect the central C−C bond, an equalization of the butadiene C−C bonds occurs in the complex. As a consequence of the low symmetry of the coordination sphere, the d orbitals of the metal center are strongly deformed. HOMO−3 and HOMO−4 are the bonding combinations of the butadiene orbital ψ^2 with the metal orbitals d_{xy} (**145**) and d_{yz} (**144**). ψ^2 is bonding with respect to the terminal C−C bonds but antibonding with respect to the central C−C bond and represents the HOMO of free butadiene (cf Figure 12). Molecular orbitals **143** and **141** represent the bonding interactions of the phosphine lone pairs with d_{yz} (**143**) and d_{xz} (**141**), respectively. MO **142** is a dppe orbital that is nonbonding with respect to the metal. All three MO's (**141**, **142**, **143**) have strong phenyl-π contributions. The LUMO (**149**) and LUMO+1 (**150**), on the other hand, are dominated by phenyl-π orbitals. The LUMO (**149**) additionally has a nonbonding $d_{x^2-y^2}$ contribution, whereas the LUMO+1 (**150**) contains a nonbonding d_{xz} contribution.

The corresponding cationic complex **2** shows a comparable MO scheme (Figure S9, Supporting Information). The SOMO **148** is metal−ligand nonbonding like the HOMO in complex **3**. The MOs **147** and **146** mediate the backbonding interactions with the ψ^3 butadiene orbitals. SOMO−3 (**145**) is equivalent to the bonding phosphine orbital **141** of **2**; the bonding combinations of the ψ^2 orbitals are located in the MOs **144** and **136**. The energetic sequence of the orbitals in **2** thus is slightly different as compared to **3**, which is due to the change in the coordination sphere, i.e., the different arrangement of the butadiene ligands.

In contrast to compounds **2** and **3**, *all* molybdenum d orbitals contribute to the metal−ligand π-bonding the homoleptic tris(butadiene) complex $[Mo(bd)_3]$ ($\mathbf{1}^{bd}$) (Figure 13).

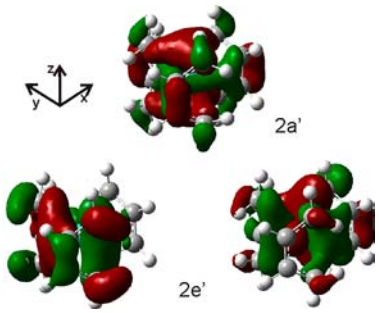

Figure 13. Highest occupied MOs of $[Mo(bd)_3]$ ($\mathbf{1}^{bd}$; cf. ref 2).

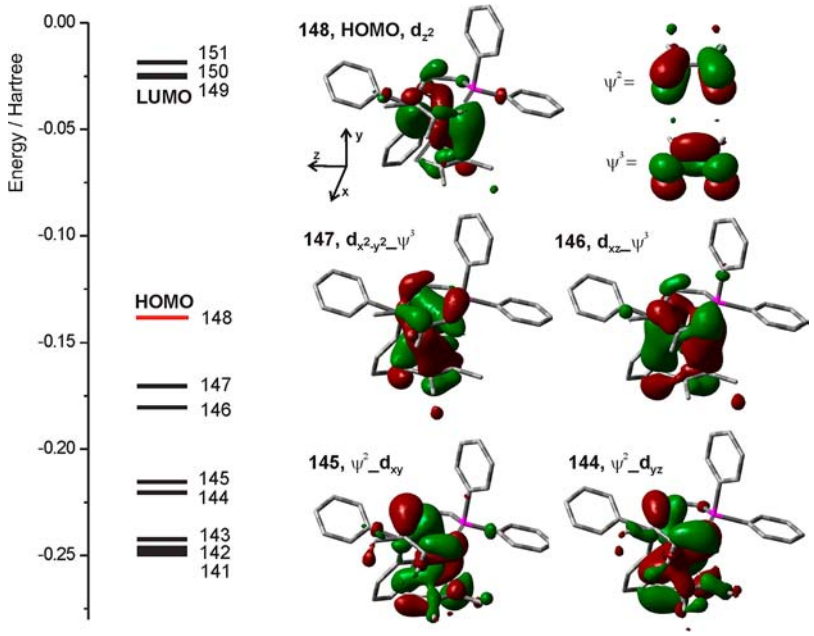

Figure 12. MO scheme of complex $[Mo(dmbd)_2(dppe)]$ (**3**).

dx.doi.org/10.1021/ic400145f | Inorg. Chem. 2013, 52, 5931−5942

Specifically, the HOMO (2a′) is the combination of d_{z^2} and ψ^3; HOMO−1 and HOMO−2 (2e′) are bonding combinations of $d_{x^2-y^2}$ and d_{xy} with and ψ^3.[2] This is similar to **2** and **3** with the exception that these heteroleptic complexes have a metal−ligand *nonbonding* orbital as the HOMO (*vide supra*). As a result, one-electron oxidation of the complex (HOMO doubly vs singly occupied) does not significantly influence the bonding situation of the butadiene ligands.

IV. SUMMARY AND CONCLUSION

In the present paper, the first oxidative ligand substitution reaction performed on molybdenum tris(2,3-dimethylbutadiene) complexes has been reported. On the basis of this reaction, the cationic complexes $[Mo(dmbd)_2(dppe)](X)$ (X = BF_4^-, PF_6^-, BPh_4^-) (**2**) have been isolated and characterized. Compounds **2** represent a new type of 17-electron molybdenum complex being coordinated by two butadiene ligands and one bidentate phosphine. By reduction of **2**, the corresponding neutral molybenum complex $[Mo(dmbd)_2(dppe)]$ (**3**) could be synthesized. Importantly, this heteroleptic complex was not directly accessible by a ligand exchange reaction of $[Mo(dmbd)_3]$. The bonding situation of the coordinated diene ligands in the heteroleptic systems as well as in the parent molybdenum trisbutadiene complexes has been investigated by a combination of spectroscopy and DFT. For the complex $[Mo(bd)_3]$ ($\mathbf{1}^{bd}$), a normal coordinate analysis has been performed. Following a procedure previously employed by us for the analysis of dinitrogen and $-NNH_x$ complexes,[31] force constants for the central and the terminal butadiene C−C bonds of 4.97 and 3.79 mdyn/Å, respectively, have been determined, reflecting the fact that the backbonding interaction predominantly involves the terminal C−C bonds of these ligands. Similar results are obtained for $\mathbf{1}^{dmbd}$ and new heteroleptic 17- and 18-electron complexes **2** and **3**, all of which approximately exhibit the same degree of backbonding. This also becomes evident from a consideration of ^1J(C−H) coupling constants at the terminal carbon atoms of the coordinated bd/dmbd ligands of $\mathbf{1}^{bd}$, $\mathbf{1}^{dmbd}$, and **3**, all of which have values around 150 Hz, corresponding to hybridizations around $sp^{2.4}$.

Seventeen-electron molybdenum complexes are rare. Their preparation by oxidation of appropriate 18-electron molybdenum complexes is, however, well established and has been applied to bis(arene) and hexaphosphine compounds.[8,32−34] In contrast to these compounds, which form stable 17-electron complexes, the one-electron oxidized counterparts of $[Mo(bd)_3]$ and $[Mo(dmbd)_3]$ easily undergo substitution reactions. The parent complexes, on the other hand, are quite unreactive. The reason for the different reactivities can be inferred from the electronic struture of $[Mo(bd)_3]$ in which all metal d orbitals contribute to the metal diene bonding.[2,35] Oxidation of the metal center thus weakens the metal−butadiene bond and renders (at least) one ligand substitutable.

The 1,3-butadiene complex $[Mo(bd)_3]$ ($\mathbf{1}^{bd}$) exhibits a different reactivity as compared to its methylated counterpart $\mathbf{1}^{dmbd}$: while $[Mo(dmbd)_3]$ could be oxidized to stable 17-electron molybdenum complexes **2** with a $[Mo(dmbd)_2(dppe)]^+$ unit, the corresponding $[Mo(bd)_2(dppe)]^+$ complex could not be isolated as a defined compound. By means of an amalgam reduction of the cationic complexes $[Mo(dmbd)_2(dppe)](X)$ (**2**), it was possible to convert to the corresponding neutral complex **3**. Both **2** and **3** were characterized by X-ray structure analysis and exhibit a similar C_2 symmetric structure. Importantly, the oxidation state has no influence on the characteristic equalization of the butadiene C−C bond lengths. These results were confirmed by vibrational spectroscopy and density functional calculations and could be explained by the electronic structure. Both in **2** and in **3**, the highest occupied molecular orbital is a metal d_{z^2} orbital with almost metal−ligand nonbonding character. Therefore, the oxidation state, particularly, the single vs double occupancy of the HOMO, has no influence on the backbonding interaction from the metal into the unoccupied orbitals of the diene ligands. However, two other metal orbitals in **2** and **3** *are* involved in a metal → backbonding interaction with the two butadiene ligands, causing a similar elongation of their C−C bonds as encountered in the homoleptic $[Mo(bd)_3]$ and $[Mo(dmbd)_3]$ complexes, where three doubly occupied metal orbitals are involved in a backbonding interaction with three butadiene ligands.

Note that in the previous discussion, no reference to the actual charge distribution in the molybdenum complexes **1**−**3** has been made. In the homoleptic complex $[Mo(bd)_3]$ ($\mathbf{1}^{bd}$), the Mo center has been assigned a charge of +IV by Kaupp et al. (*vide supra*). The two electrons in the metal-based d_{z^2}-type HOMO of **3** would correspondingly give rise to a d^2 configuration. Ionization from this orbital would then lead to a d^1 configuration, i.e., a Mo(+V) charge state, in **2**. As found computationally in previous d^2 vs d^1 comparisons,[36] this entails only little structural consequence, in full agreement with the results of this paper.

■ ASSOCIATED CONTENT

Ⓢ Supporting Information

Normal modes of $[Mo(bd)_3]$; vibrational spectra of $[Mo(dmbd)_3]$; magnetic data of **2**; NMR spectra and structures of $\mathbf{1}^{bd}$, $\mathbf{1}^{dmbd}$, and **3**; and MO scheme of **2**. This material is available free of charge via the Internet at http://pubs.acs.org.

■ AUTHOR INFORMATION

Corresponding Author

*Tel.: ++49 (0)431 880 1410. Fax: ++49 (0)431 880 1520. E-mail: ftuczek@ac.uni-kiel.de.

Notes

The authors declare no competing financial interest.

■ ACKNOWLEDGMENTS

F.T. thanks CAU Kiel and the State of Schleswig-Holstein for support of this research.

■ REFERENCES

(1) Skell, P. S.; van Dam, P. M.; Selvon, M. P. *J. Am. Chem. Soc.* **1974**, *96*, 626−627.
(2) Kaupp, M.; Kopf, T.; Murso, A.; Stalke, D.; Strohmann, C.; Hanks, J. R.; Cloke, F. G. N.; Hitchcock, P. B. *Organometallics* **2002**, *21*, 5021−5028.
(3) Tate, D. P.; Knipple, W. R.; Augl, J. M. *Inorg. Chem.* **1962**, *1*, 433−434.
(4) Fischer, E. O.; Kögler, H. P.; Kuzel, P. *Chem. Ber.* **1960**, *93*, 3006−3013.
(5) Fontaine, X. L. R.; Kennedy, J. D.; Shaw, B. L.; Vila, J. M. *J. Chem. Soc., Dalton Trans.* **1987**, 2401−2405.
(6) Green, M. L. H.; Mitchard, L. C.; Silverthorn, W. E. *J. Chem. Soc. A* **1971**, 2929−2931.
(7) Poli, R.; Krueger, S. T.; Mattamana, S. P. *Inorg. Synth.* **1998**, *32*, 198−203.
(8) Silverthorn, W. E. *Inorg. Chem.* **1979**, *18*, 1835−1838.

(9) Zhu, A. G.; Tanski, J. M.; Churchill, D. G.; Janak, K. E.; Parkin, G. *J. Am. Chem. Soc.* **2002**, *124*, 13658−13659.
(10) Buccella, D.; Janak, K. E.; Parkin, G. *J. Am. Chem. Soc.* **2008**, *130*, 16187−16189.
(11) Sattler, A.; Zhu, G.; Parkin, G. *J. Am. Chem. Soc.* **2009**, *131*, 7828−7838.
(12) Gausing, W.; Wilke, G. *Angew. Chem., Int. Ed.* **1981**, *20*, 186−187.
(13) Startsev, A. N.; Bogdanovic, B.; Bönnemann, H.; Rodin, V. N.; Yermakov, Y. I. *J. Chem. Soc., Chem. Comm.* **1986**, 381−382.
(14) Brookhart, M.; Cox, K.; Cloke, F. G. N.; Green, J. C.; Green, M. L. H.; Hare, P. M.; Bashkin, J.; Derome, A. E.; Grebenik, P. D. *J. Chem. Soc., Dalton Trans.* **1985**, 423−433.
(15) Galindo, A.; Gutierrez, E.; Monge, A.; Paneque, M.; Pastor, A.; Perez, P. J.; Rogers, R. D.; Carmona, E. *J. Chem. Soc., Dalton Trans.* **1995**, 3801−3808.
(16) Becke, A. D. *J. Chem. Phys.* **1993**, *98*, 5648−5652.
(17) Dunning, T. H.; Hay, P. J. In *Modern Theoretical Chemistry*; Plenum Press: New York, 1976.
(18) (a) Hay, P. J.; Wadt, W. R. *J. Chem. Phys.* **1985**, *82*, 270−283. (b) Wadt, W. R.; Hay, P. J. *J. Chem. Phys.* **1985**, *82*, 284−298. (c) Hay, P. J.; Wadt, W. R. *J. Chem. Phys.* **1985**, *82*, 299−310.
(19) Frisch, M. J.; Trucks, G. W.; Schlegel, H. B.; Scuseria, G. E.; Robb, M. A.; Cheeseman, J. R.; Montgomery, J. A., Jr.; Vreven, T.; Kudin, K. N.; Burant, J. C.; Millam, J. M.; Iyengar, S. S.; Tomasi, J.; Barone, V.; Mennucci, B.; Cossi, M.; Scalmani, G.; Rega, N.; Petersson, G. A.; Nakatsuji, H.; Hada, M.; Ehara, M.; Toyota, K.; Fukuda, R.; Hasegawa, J.; Ishida, M.; Nakajima, T.; Honda, Y.; Kitao, O.; Nakai, H.; Klene, M.; Li, X.; Knox, J. E.; Hratchian, H. P.; Cross, J. B.; Bakken, V.; Adamo, C.; Jaramillo, J.; Gomperts, R.; Stratmann, R. E.; Yazyev, O.; Austin, A. J.; Cammi, R.; Pomelli, C.; Ochterski, J. W.; Ayala, P. Y.; Morokuma, K.; Voth, G. A.; Salvador, P.; Dannenberg, J. J.; Zakrzewski, V. G.; Dapprich, S.; Daniels, A. D.; Strain, M. C.; Farkas, O.; Malick, D. K.; Rabuck, A. D.; Raghavachari, K.; Foresman, J. B.; Ortiz, J. V.; Cui, Q.; Baboul, A. G.; Clifford, S.; Cioslowski, J.; Stefanov, B. B.; Liu, G.; Liashenko, A.; Piskorz, P.; Komaromi, I.; Martin, R. L.; Fox, D. J.; Keith, T.; Al-Laham, M. A.; Peng, C. Y.; Nanayakkara, A.; Challacombe, M.; Gill, P. M. W.; Johnson, B.; Chen, W.; Wong, M. W.; Gonzalez, C.; Pople, J. A. *Gaussian 03*, revision B.03; Gaussian, Inc.: Pittsburgh, PA, 2003.
(20) *GaussView*, 3.07; Gaussian, Inc.: Pittsburgh, PA, 2003.
(21) Peterson, M. R.; McIntosh, D. F. *QCPE program 576*; Indiana University: Bloomington, IN, 1988.
(22) Nelder, J. A.; Mead, R. *Comput. J.* **1965**, *7*, 308−313.
(23) Allouche, A.; Pourcin, J. *Spectrochim. Acta, Part A* **1993**, *49*, 571−580.
(24) Ellis, R.; Henderson, R. A.; Hills, A.; Hughes, D. L. *J. Organomet. Chem.* **1987**, C6−C10.
(25) Tang, W.; Zhang, X.; Bally, T. *J. Phys. Chem.* **1993**, *97*, 4365−4372.
(26) Bogdanovic, B.; Bönnemann, H.; Goddard, R.; Startzev, A.; Wallis, J. M. *J. Organomet. Chem.* **1986**, *299*, 347−355.
(27) Yun, S. S.; Kang, S. K.; Suh, I.-H.; Choi, Y. D.; Chang, I. S. *Organometallics* **1991**, *10*, 2509−2512.
(28) Nakayama, Y.; Saito, H.; Ueyama, N.; Nakamura, A. *J. Organomet. Chem.* **2001**, *627*, 221−225.
(29) Benn, R.; Brevard, C.; Rufiinska, A.; Schroth, G. *Organometallics* **1987**, *6*, 938−942.
(30) Newton, M. D.; Schulman, J. M.; Manus, M. M. *J. Am. Chem. Soc.* **1974**, *96*, 17−23.
(31) (a) Lehnert, N.; Tuczek, F. *Inorg. Chem.* **1999**, *38*, 1659−1670. (b) Horn, K. H.; Lehnert, N.; Tuczek, F. *Inorg. Chem.* **2003**, *42*, 1076−1086. (c) Studt, F.; MacKay, B. A.; Fryzuk, M. D.; Tuczek, F. *J. Am. Chem. Soc.* **2004**, *126*, 280−290. (d) Stephan, G. C.; Peters, G.; Lehnert, N.; Habeck, C. M.; Näther, C.; Tuczek, F. *Can. J. Chem.* **2005**, *83*, 385−402. (e) Horn, K. H.; Böres, N.; Lehnert, N.; Mersmann, K.; Näther, C.; Peters, G.; Tuczek, F. *Inorg. Chem.* **2005**, *44*, 3016−3030.
(32) Calucci, L.; Cloke, F. G. N.; Englert, U.; Hitchcock, P. B.; Pampaloni, G.; Pinzino, C.; Puccini, F.; Volpe, M. *Dalton Trans.* **2006**, 4228−4234.
(33) Domrachev, G. A.; Shevelev, Y. A.; Cherkasov, V. K.; Markin, G. V.; Fukin, G. K.; Khorshev, S. Y.; Kaverin, B. S.; Karnatchevich, V. L. *Russ. Chem. Bull., Int. Ed* **2004**, *53*, 2056−2059.
(34) Cloke, F. G. N.; Fyne, P. J.; Gibson, V. C.; Green, M. L. H.; Ledoux, M. J.; Perutz, R. N. *J. Organomet. Chem.* **1984**, *277*, 61−73.
(35) Green, J. C.; Kelly, M. R.; Grebenik, P. D.; Briant, C. E.; McEvoy, N. A.; Mingos, D. M. P. *J. Organomet. Chem.* **1982**, *228*, 239−247.
(36) Kaupp, M. *Angew. Chem., Int. Ed.* **2001**, *40*, 3534−3565.